Development of Wide Color-Gamut Green OLED Devices for Adobe and BT2020 Requirements

Guomeng Li[1], Baoyu Li[1], Minghan Cai[1], Mihwa Ha[2], Wonjun Song[2], Ying Shen[2], Xiujian Zhu[2], Xiaoqin Jia[3], Yilang Li[3], Song Liu[3], Yuewei Zhang[4], Dongdong Zhang[4], Lian Duan[4]

[1]Beijing Visionox Technology Co., Ltd., Beijing, 100089, P. R. China

[2]Kunshan Govisionox Optoelectronics Co., Ltd. (Visionox's Affiliated Company), Kunshan, Jiangsu, 215300, P. R. China

[3]Beijing Eternal Material Technology Co., Ltd., 100089, Beijing, P. R. China

[4]Tsinghua University, Department of Chemistry, Beijing, 100089, P. R. China

Abstract

The current commercial panel OLED products are mainly meet DCI-P3 gamut display, lacking the development of display technology with wide color gamut. In this paper, we fabricated a series of pTSF green devices, which can meet Adobe and BT2020 requirements. The optimal pTSF devices which exhibit excellent performance by distribution trend at CIEx < 0.21, and pTSF devices show higher color purity, better efficiency and better lifetime than existing phosphporescent devices. Showing the advantages in wide color gamut display.

Author Keywords

Organic light-emitting diode; Phosphor-assisted TADF sensitized fluorescence; Wide color gamut; High color purity; High efficiency; Long lifetime;

1. Introduction

Active Matrix Organic Light Emitting Diode (AMOLED) technology is known for its superior display performance like high contrast, high resolution, ultra-thin, flexibe. which is increasingly being adopted in various terminal products. As the demand for screen display quality continues to rise, wide color gamut OLED displays (such as Adobe and BT2020 standards) are showing broad application prospects across multiple fields. In the consumer electronics sector, wide color gamut OLED technology can provide smartphones, tablets, televisions, and monitors with more vibrant colors, significantly enhancing the user experience. In professional display equipment, wide color gamut OLED technology enables precise color reproduction in film production and graphic design, improving the quality of the final product. In virtual reality (VR) and augmented reality (AR) devices, wide color gamut OLED technology provides high resolution, high refresh rate, and high color reproduction displays, achieving more realistic and immersive experiences. These applications demonstrate the extensive potential of wide color gamut OLED devices in multiple fields. As display technology continues to advance, wide color gamut OLED technology is expected to bring revolutionary changes to many industries. One of the major challenges in developing wide color gamut OLEDs is to achieve high color purity and high performance of OLED devices. Existing phosphorescent technology is limited by the inherent broad full width at half maximum (FWHM) and significant shoulder peaks in emission spectrum of phosphorescent materials, which result in difficult to apply in wide color gamut OLED development. While recently there are many researches have focused on fluorescent emitters with narrow emission spectra[1-10], but there is a lack of studies on how to utilize this type of material into commercial mass production device structures. Current performance reported usually existing a trade-off among efficiency, lifetime and color purity, leading hard to meet the requirements of commercial products. Previously our team reported the development of Phosphor-assisted TADF sensitized fluorescence (pTSF) technology[11], and we are the first to evaluate pTSF technology under the device structure in mass production system[12-13]. Phosphorescent material is used as phosphor assistant sensitizer to transfer energy to narrow spectrum fluorescent materials in pTSF mechanism, which can achieve 100% exciton utilization. Compared to existing phosphorescent technology, pTSF technology provides a range of performance advantages such as high color purity, high efficiency, long lifetime, and low cost. Recently we have made new progress in pTSF technology. In this work, we fabricated a series of green pTSF devices which meet the wide color gamut requirements of Adobe and BT2020 standards. We investigated the collocation of host material, phosphor assistant sensitizer material and narrow-spectrum fluorescent material in pTSF devices and analyzed pTSF devices performance. The optimized pTSF devices show superior performance compared to commercial phosphorescent devices by distribution trend at CIEx＜0.21, demonstrating better color purity, efficiency, and device lifetime. These findings indicate promising applications of pTSF technology in the wide color gamut display field.

2. Experimental details

2.1 Device Fabrication

Substrates were rinsed with cleaning solvents and followed by exposure to ambient UV-Ozone. All of the functional layers were deposited by vacuum thermal evaporation equipment with a base pressure of 10^{-5} pa. The thickness was monitored by INFICON film thickness detection system and calibrated by SEMILAB spectroscopic ellipsometry. The samples are encapsulated under nitrogen atmosphere with glass lids directly after preparation.

The architecture of the bottom device is: Anode/hole injection layer (HIL)/hole transporting layer (HTL)/electron blocking layer (EBL)/EML/hole blocking layer (HBL)/electron transporting layer (ETL)/electron injection layer (EIL)/non-transparent cathode.

The architecture of the top device is: Anode/hole injection layer (HIL)/hole transporting layer (HTL)/electron blocking layer (EBL)/EML/hole blocking layer (HBL)/electron transporting layer (ETL)/electron injection layer (EIL)/transparent cathode/capping layer (CPL).

2.2 Testing Equipment

All the measurement of the current voltage characteristics of the devices were performed with a Keithley 2400 source meter (Keithley Instruments, Inc., Solon, OH, USA). The luminance and spectrum of the devices were recorded with a PR-788 Spectra Scan

ISSN 0097-996X/25/5601-0656-$1.00 © 2025

colorimeter (Photo Research, Inc., Chatsworth, CA, USA). The lifetime of the devices were measured with a Keithley 3706A (Keithley Instruments, Inc, Solon, OH, USA) of CRYSCO testing equipment at fixed current density. All efficiency and lifetime data are presented in a percentage manner relative to designated reference (100%). The capacitance of the devices were measured by the Keithley 4200-SCS (Semiconductor Characterization System) probe station at the frequency of 10K Hz.

3. Results and Discussions

3.1 Comparison of OLED characteristics between phosphorescent and pTSF bottom-emitting devices

Firstly, we prepared a series of bottom-emission devices, these devices share common functional layers and identical anode and cathode structures. The differences lie in their emitting layer compositions. Device A is a phosphorescent device with an emitting layer composed of host material and phosphorescent dopant PD1, which is currently a commercial mass production phosphorescent device with DCI-P3 color gamut. Device B is also a phosphorescent device, but its emitting layer consists of host material and phosphorescent dopant PD2. Device C is a pTSF (Phosphor-assisted TADF sensitized fluorescence) device, As shown in **Figure 1**, which emitting layer consists of host material, phosphor assistant sensitizer dopant PD1, and narrow spectrum fluorescent material FD1, compared to Device A, the key difference is the introduction of the narrow spectrum fluorescent material FD1 into the emissive layer, these three materials are evaporated into the emissive layer using a three source co evaporation method. Through the pTSF energy transfer mechanism, phosphorescent material is used as phosphor assistant sensitizer to transfer energy to narrow spectrum fluorescent material, sensitized fluorescent materials emission is achieved, which can achieve 100% exciton utilization. Using the fluorescent material for emission fundamentally improves the issue of broad spectral shoulder peaks caused by the inherent large stokes shift of phosphorescence material. Device D is also a pTSF device. Compared to Device B, Device D incorporates a narrow-spectrum dye FGD1 into the emissive layer, with host material and phosphorescent material PGD2. The device structures and main OLED characteristics of four devices are represented in **Figure 2a-2d** and **Table 1**, the driving voltages (at 10 mA/cm^2) of pTSF devices (Device C and Device D) are basically consistent with the phosphorescent device (Device A and Device B), which indicates that the FD material does not exhibit significant carrier trapping in he pTSF devices. Device B exhibits a narrower emission spectrum, decreasing from 53 nm to 29 nm compared to Device A additionally with the emission peak is blue-shifted by

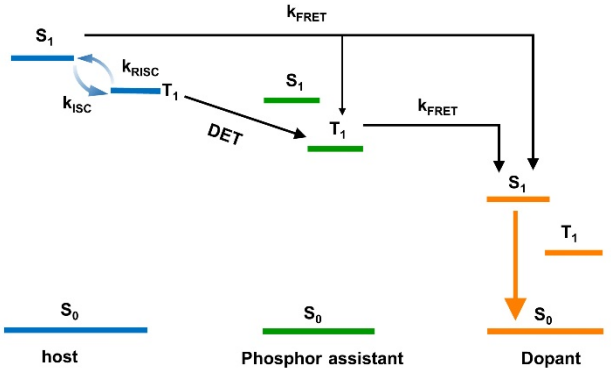

Figure 1 Diagram of the exciton transfer process in the pTSF system

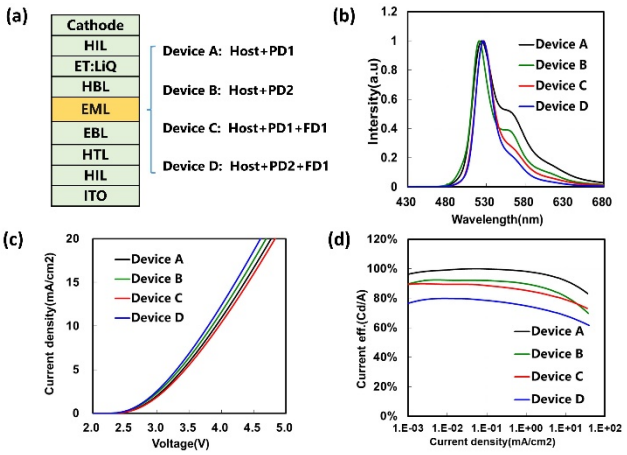

Figure 2 (a) Bottom-emission device structure of series devices, (b) Normalized bottom EL spectra of Device A, Device B, Device C and Device D, (c) Current density-voltage, (d) Normalization current efficiency-current density.

Table 1 Main performance of Bottom Device A, Device B, D evice C and Device D at current density of 10 mA/cm^2

Device No.	CIE	Main Peak (nm)	FWHM (nm)	Vd (V)	Eff. (cd/A)
Device A	(0.334, 0.628)	524	53	3.90	100%
Device B	(0.297, 0.650)	521	29	3.85	88.3%
Device C	(0.283, 0.676)	526	27	3.96	85.9%
Device D	(0.256, 0.699)	526	26	3.80	74.1%

3 nm. However, the efficiency and lifetime of Device B are somewhat reduced compared to those of Device A. As can be seen, Device C shows a significant narrowing of the emission spectrum compared to Device A, decreasing FWHM from 53 nm to 27 nm. Additionally, there is a marked improvement in the right trailing part of the EL spectrum. And Device C exhibits a narrower emission wavelength and better suppression of the shoulder peak of the EL spectrum compared to Device B. When comparing Device B with Device D, Device D demonstrates a narrower FWHM and a better right shoulder peak profile. Additionally, when comparing Device C and Device D, it is evident that using different phosphorescent materials PGD2 to sensitize the same fluorescent material FGD1 results in a further reduction in the FWHM of Device D. This is because the PGD2 material used in Device D has a bluer and narrower spectrum, leading to more efficient energy transfer to FGD1 under the pTSF sensitization mechanism. This improved energy transfer further suppresses the intrinsic emission of the phosphorescent material, resulting in more light being emitted by the fluorescent material FGD1. This is crucial for achieving wide color gamut pTSF device systems. The excellent bottom-emission performance of Device C and Device D also suggests superior performance top-emission devices for wide color gamut.

3.2 Comparison of OLED characteristics between phosphorescent and pTSF top-emitting devices

To study the characteristics of the materials and device configurations, we further fabricated top-emission Devices E, F, G,

and H. The device structures are shown in **Figure 3a.** Devices E and F are phosphorescent devices, while devices G and H are pTSF devices. It can be observed that the emissive layer materials of devices E, F, G, and H are identical to those of Devices A, B, C, and D, respectively. **Figure 3b-3d** show the normalized EL spectra, current density-voltage curves, normalization current efficiency-luminance curves of Device E, F, G and H, and the key performance metrics are collected in **Table 2**, it can be observed that the phosphorescent Device E and Device F have relatively broad full widths at half maximum (FWHM). And Device E has the largest FWHM and shoulder peak among the four devices. Device E uses phosphorescent material PD2 for emission, exhibiting DCI-P3 chromaticity with a color point CIEx of 0.245 and FWHM of 28 nm. In comparison, Device F which uses phosphorescent material PD2 for emission, shows a blue-shifted emission peak with FWHM of 25 nm and a color point CIEx of 0.207 which meet Adobe chromaticity. The current efficiency and lifetime of device F are lower than those of device E, which due to along with the emission wavelength blue-shifts of phosphorescent materials, the further increase in the T1 energy level will lead to more severe triplet-triplet annihilation (TTA) and triplet-polaron annihilation (TPA) quenching issues, which are detrimental to achieving high color purity and high-performance OLED devices. Device G is a pTSF device, the emission spectrum of Device G is significantly narrowed compared to Device E, and the device performance is markedly improved. The emissive layer of Device G employs the pTSF mechanism, transfer energy to the narrow spectrum fluorescent material for emission. As we can see, we used phosphorescent material PD1 with DCI-P3 chromaticity to sensitize the narrow spectrum fluorescent material FD1, achieving an Adobe chromaticity emission with a color point CIEx of 0.208. Additionally, the current efficiency and lifetime of Device G are significantly enhanced compared to Device E, in particular with the lifetime improving by over 30%. This improvement is attributed to the pTSF energy transfer mechanism, where the emission occurs in the excited state of the fluorescent material, which can significantly reduce the exciton lifetime in the emissive layer compared to phosphorescent emission, allowing exciton to return to the ground state and emit light quickly, and the reduction in emitting molecular excited state lifetime also contributes to improved device lifetime. Furthermore, when comparing Device G with Device F, both devices exhibit similar color points. However, in terms of efficiency and lifetime, Device G shows substantial improvements over device F. Which highlights the performance advantages of pTSF devices over phosphorescent devices. Device H is also a pTSF device which shows further optimization in color purity compared to Devices G. Device H achieves a color point CIEx of 0.175 with a FWHM of 21 nm, demonstrating high color purity that nearly meets the BT2020 requirements. This improvement is due to the use of a bluer phosphorescent material GD2 in the emitting layer of Device H, which serves as a phosphor assistant sensitizer, the phosphorescent material GD2 and the fluorescent material FD1 have better absorption and emission spectra overlap, leading to more efficient energy transfer between each other and reduce unnecessary phosphorescent self-emission, further enhancing the color purity of the device. Additionally, the current efficiency and lifetime of Device H are significantly better than phosphorescent Device F, even comparable with the commercial mass production phosphorescent Device E with DCI-P3 chromaticity. From the above performance comparisons, it is clear that pTSF devices have better color purity, higher efficiency, and longer lifetimes compared to phosphorescent devices which are obtained by combining the molecular design optimization of narrow spectral materials and device structure optimization.

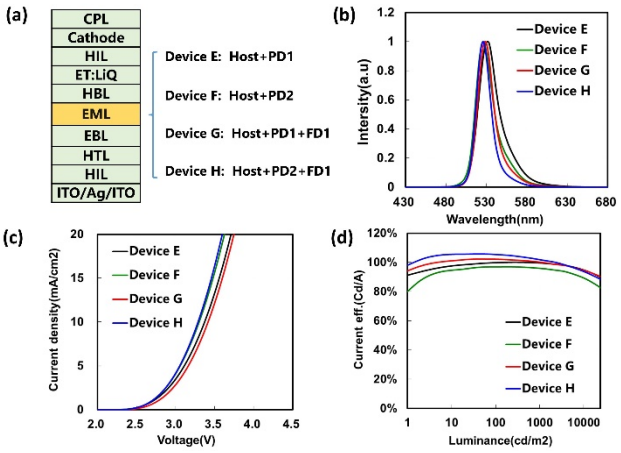

Figure 3 (a) Top-emission device structure of series devices, (b) Normalized top EL spectra of Device E, Device F, Device G and Device H, (c) Current density-voltage, (d) Normalization current efficiency-luminance.

Table 2 Main performance of Device E, Device F, Device G and Device H at luminance of 12000 nit.

Device No.	CIE	Main Peak (nm)	FWHM (nm)	Vd (V)	Eff. (cd/A)	LT95 @15J (h)
Device E	(0.245, 0.720)	531	28	3.17	100%	100%
Device F	(0.207, 0.743)	526	25	3.13	93.8%	75%
Device G	(0.208, 0.748)	527	23	3.21	101%	132%
Device H	(0.175, 0.769)	526	21	3.11	98.8%	109%

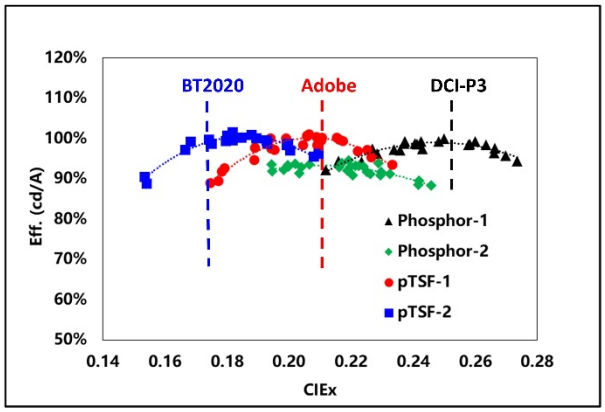

Figure 4 Efficiency-CIEx mapping of series top-emitting devices at the luminance of 12000nits.

The EBL thickness in top-emission OLED devices of the four series of devices (phosphor-1 device with Host+PD1, phosphor-2 device with Host+PD2, pTSF-1 devices with Host+PD1+FD1 and pTSF-2 devices with Host+PD2+FD1) were adjusted to fine-tune the CIEx values, and the efficiency-CIEx mapping is depicted in **Figure.4**. As shown in **Figure 4**, the phosphor-1 series devices exhibit a central efficiency color point around 0.250, meeting the chromaticity requirements of DCI-P3. The phosphor-2 series devices have a central efficiency color point around 0.21, with a noticeable decrease in efficiency compared to the phosphor-1 series devices. The pTSF-1 series devices have a central efficiency color point around 0.205, which satisfies the Adobe color gamut display

requirements. The pTSF-2 series devices have a central efficiency color point around 0.178, representing the best chromaticity performance among this four series devices and potentially meeting the BT2020 chromaticity requirements. The efficiency performance of both the pTSF-1 and pTSF-2 series devices is also favorable, performing on par with or even exceeding the commercial mass production DCI-P3 phosphorescent devices. It is evidently the optimized pTSF devices show superior performance compared to commercial phosphorescent devices by distribution trend at CIEx＜0.21, This makes pTSF devices particularly advantageous for wide color gamut OLED applications.

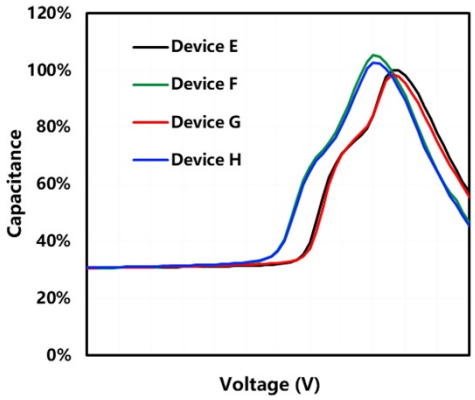

Figure 5 Capacitance-Voltage diagrams of Device E, Device F, Device G and Device H.

The capacitance of OLED devices has received widespread attention as it is considered to be related to device reliability and some aspects of panel image quality. To investigate the impact of introducing new narrow spectrum fluorescent material on the capacitance of pTSF devices, we tested the capacitance of Device E, Device F, Device G, and Device H. As shown in **Figure 5**, it can be observed that the peak capacitance of Device E and Device F is close. When comparing the peak capacitance of Device E to 100%, the peak capacitance of Device F is 105.3%, slightly higher than that of Sevice E, the capacitance onset of Device F occurs slightly earlier than that of Device E, which may be attributed to the strong carrier trapping characteristics of phosphorescent material PD2, facilitating charge injection into the emissive layer. When comparing Device E and Device G, the capacitance peak shape and value are essentially consistent, and the capacitance characteristics of devices F and H are also similarly. This indicates that the introduction of the narrow spectrum fluorescent material FD1 in Device G and Device H has minimal impact on the device capacitance. Combined with the previous current-voltage performance, it can be inferred that the introduced FD1 material does not exhibit significant carrier trapping compared to the original phosphorescent devices, there are no significant changes in turn on voltage, operating voltage, or capacitance. Beyond the performance metrics we discussed before, we have also evaluated other tests for the mass production feasibility of pTSF technology, includes assessments of device temperature dependent IV stability, high temperature operational stability, view angle characteristics, and the stability of doping concentration variations in the production line evaporation sources. pTSF technology performs well in all these aspects evaluations, indicating that pTSF technology is ready for mass production applications.

3.3 Exploration of wide color gamut pTSF devices

Currently, pTSF technology has demonstrated significant performance advantages over existing phosphorescent technology. We have also investigated a variety of pTSF material combinations in device, optimizing the host materials, phosphorescent materials, and narrow spectrum fluorescent materials to further refine series devices of pTSF-3, pTSF-4, and pTSF-5. As shown in **Figure 6**, compared to the reference phosphorescent devices phosphor-2, the pTSF series devices exhibit excellent wide-color-gamut OLED performance, with central CIEx color points reaching the level of 0.17 or even lower than it, matching even exceeding the BT2020 color gamut requirements, which is difficult to achieve by phosphorescent devices. Additionally, the efficiency of the pTSF devices is notably higher than that of the reference phosphorescent devices. These findings further indicate promising applications of pTSF technology in the wide color gamut display field.

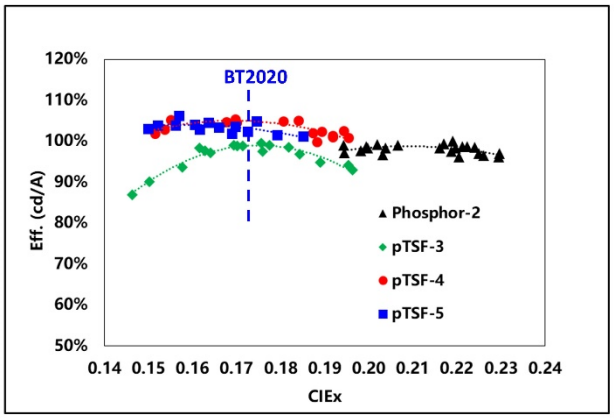

Figure 6 Efficiency-CIEx mapping of series pTSF top-emitting devices at the luminance of 12000nits.

4. Conclusions and Outlook

In summary, we have fabricated a series of pTSF devices and compared characteristics with corresponding phosphorescent devices, the pTSF devices exhibit comparable or even higher current efficiency compared to phosphorescent devices, represent a significant improvement exceeding more than 30% in device lifetime. The color purity of pTSF devices have been extended from DCI-P3 to Adobe and BT2020 color gamuts. Moreover, the turn-on voltage, operating voltage, and capacitance of the pTSF technology have not been significantly affected. These results demonstrate that pTSF technology offers advantages such as narrow spectrum emission, high color purity, high efficiency, long device lifetime. Therefore, this technology shows great technical advantages and good application potential, especially for the development of high performance and high color purity OLED system to meet the wide color gamut requirements.

5. Acknowledgement

We want to thank Tsinghua University Department of Chemistry, Beijing Eternal Material Technology Co., Ltd. and Visionox Technology Co., Ltd. for theoretical guidance, material preparation, device fabrication, financial and technical support. And we are grateful for efforts from all colleagues.

6. References

[1] Zhang, Y., Zhang, D., Wei, J., Liu, Z., Lu, Y., et al. (2019). Multi-Resonance induced thermally activated delayed fluorophores for narrowband green OLEDs. *Angewandte Chemie International Edition*, *58*(47), 16912–16917. https://doi.org/10.1002/anie.201911266

[2] Song, X., Zhang, D., Zhang, Y., Lu, Y., et al. (2020). Strategically Modulating Carriers and Excitons for Efficient and Stable Ultrapure-Green Fluorescent OLEDs with a Sterically Hindered BODIPY Dopant. *Advanced Optical*

Materials, *8*(15). https://doi.org/10.1002/adom.202000483

[3] Yin, C., Zhang, D., Zhang, Y., Lu, Y., Wang, R., Li, G., et al. (2020). High-Efficiency Narrow-Band Electro-Fluorescent Devices with Thermally Activated Delayed Fluorescence Sensitizers Combined Through-Bond and Through-Space Charge Transfers. *CCS Chemistry*, *2*(4), 1268-1277. https://doi.org/10.31635/ccschem.020.202000243

[4] Fan, T., Zhu, S., Cao, X., Liang, X., Du, M., et al. (2023). Tailored Design of π-Extended Multi-Resonance Organoboron using Indolo[3,2-b]Indole as a Multi-Nitrogen Bridge. *Angewandte Chemie International Edition*, *62*(48). https://doi.org/10.1002/anie.202313254

[5] Wu, Z., Xin, Y., Lu, C., Huang, W., Xu, H., Liang, X., et al. (2023). Precise Regulation of Multiple Resonance Distribution Regions of a B,N-Embedded Polycyclic Aromatic Hydrocarbon to Customize Its BT2020 Green Emission. *Angewandte Chemie International Edition*, *63*(7). https://doi.org/10.1002/anie.202318742

[6] Liang, L., Qu, C., Fan, X., Ye, K., et al. (2023). Carbonyl- and Nitrogen-Embedded Multi-Resonance Emitter with Ultra-Pure Green Emission and High Electroluminescence Efficiencies. *Angewandte Chemie International Edition*, *63*(4). https://doi.org/10.1002/anie.202316710

[7] Wang, Q., Xu, Y., Huang, T., Qu, Y., Xue, J., et al. (2023). Precise Regulation of Emission Maxima and Construction of Highly Efficient Electroluminescent Materials with High Color Purity. *Angewandte Chemie International Edition*, *62*(19). https://doi.org/10.1002/anie.202301930

[8] Liu, J., Zhu, Y., Tsuboi, T., Deng, C., Lou, W., et al. (2022). Toward a BT.2020 green emitter through a combined multiple resonance effect and multi-lock strategy. *Nature Communications*, *13*(1). https://doi.org/10.1038/s41467-022-32607-3

[9] Zhang, Y., Li, G., Wang, L., Huang, T., Wei, J., et al. (2022). Fusion of Multi-Resonance Fragment with Conventional Polycyclic Aromatic Hydrocarbon for Nearly BT.2020 Green Emission. *Angewandte Chemie International Edition*, *134*(24). https://doi.org/10.1002/ange.202202380

[10] Lei, B., Huang, Z., Li, S., Liu, J., et al. (2023). Medium-Ring Strategy Enables Multiple Resonance Emitters with Twisted Geometry and Fast Spin-Flip to Suppress Efficiency Roll-Off. *Angewandte Chemie International Edition*, *135*(12). https://doi.org/10.1002/ange.202218405

[11] Yin, C., Zhang, Y., Huang, T., Duan, L., Zhang, D., et al. (2022). Highly efficient and nearly roll-off–free electrofluorescent devices via multiple sensitizations. *Sci. Adv.* 8(30). https://doi.org/10.1126/sciadv.abp9203.

[12] Li, G., Li, B., Zhang, D., Liu, B., Li, M., Song, W., et al. (2023). High Efficiency and High Color Purity Green OLEDs with Narrow Spectra Emission. *International Conference on Display Technology 2023* (Vol. 54, Issue S1, p. 174). https://doi.org/10.1002/sdtp.16256

[13] Li, G., Zhang, D., Li, B., Cai, M., Wang, H., Song, W. et al. (2024). High Performance and High Color Purity Green OLEDs with Narrow Spectra Emission. *SID 2024 DIGEST*, 2150. https://doi.org/10.1002/sdtp.18032